Accepted Manuscript

New naphthalene whole-cell bioreporter for measuring and assessing naphthalene in polycyclic aromatic hydrocarbons contaminated site

Yujiao Sun, Xiaohui Zhao, Dayi Zhang, Aizhong Ding, Cheng Chen, Wei E. Huang, Huichun Zhang

PII: S0045-6535(17)31248-1

DOI: 10.1016/j.chemosphere.2017.08.027

Reference: CHEM 19725

To appear in: *ECSN*

Received Date: 17 April 2017

Revised Date: 22 July 2017

Accepted Date: 7 August 2017

Please cite this article as: Sun, Y., Zhao, X., Zhang, D., Ding, A., Chen, C., Huang, W.E., Zhang, H., New naphthalene whole-cell bioreporter for measuring and assessing naphthalene in polycyclic aromatic hydrocarbons contaminated site, *Chemosphere* (2017), doi: 10.1016/j.chemosphere.2017.08.027.

New naphthalene whole-cell bioreporter for measuring and assessing naphthalene in polycyclic aromatic hydrocarbons contaminated site

Yujiao Sun[a], Xiaohui Zhao[a,b*], Dayi Zhang[c], Aizhong Ding[a], Cheng Chen[a], Wei E. Huang[d], Huichun Zhang[a].

[a] College of Water Sciences, Beijing Normal University, Beijing, 100875, PR China

[b] Department of Water Environment, China Institute of Water Resources and Hydropower Research, Beijing, 100038, China

[c] Lancaster Environment Centre, Lancaster University, Lancaster, LA1 4YQ, UK

[d] Kroto Research Institute, University of Sheffield, Sheffield, S3 7HQ, United Kingdom

Corresponding author

Dr Xiaohui Zhao

[a] College of Water Sciences, Beijing Normal University, Beijing 100875, P. R. China

[b] Department of Water Environment, China Institute of Water Resources and Hydropower Research, Beijing, 100038, China

E-mail: zhaoxiaocunforever@mail.bnu.edu.cn

Abstract

A new naphthalene bioreporter was designed and constructed in this work. A new vector, pWH1274_Nah, was constructed by the Gibson isothermal assembly fused with a 9 kb naphthalene-degrading gene nahAD (*nahAa nahAb nahAc nahAd nahB nahF nahC nahQ nahE nahD*) and cloned into *Acinetobacter* ADPWH_lux as the host, capable of responding to salicylate (the central metabolite of naphthalene). The ADPWH_Nah bioreporter could effectively metabolize naphthalene and evaluate the naphthalene in natural water and soil samples. This whole-cell bioreporter did not respond to other polycyclic aromatic hydrocarbons (PAHs; pyrene, anthracene, and phenanthrene) and demonstrated a positive response in the presence of 0.01 μM naphthalene, showing high specificity and sensitivity. The bioluminescent response was quantitatively measured after a 4 h exposure to naphthalene, and the model simulation further proved the naphthalene metabolism dynamics and the salicylate-activation mechanisms. The ADPWH_Nah bioreporter also achieved a rapid evaluation of the naphthalene in the PAH-contaminated site after chemical spill accidents, showing high consistency with chemical analysis. The engineered *Acinetobacter* variant had significant advantages in rapid naphthalene detection in the laboratory and potential *in situ* detection. The state-of-the-art concept of cloning PAHs-degrading pathway in salicylate bioreporter hosts led to the construction and assembly of high-throughput PAH bioreporter array, capable of crude oil contamination assessment and risk management.

Keywords: Naphthalene; whole-cell bioreporter; *Acinetobacter baylyi*; Gibson cloning; polycyclic aromatic hydrocarbons (PAHs)

1. Introduction

Polycyclic aromatic hydrocarbons (PAHs), a group of persistent organic pollutants, exist extensively in subsurface environments (Wilcke 2000). PAHs have been designated by the US Environmental Protection Agency (US EPA) as priority pollutants because of their possible carcinogenicity and toxicity to humans and animals (Boffetta et al. 1997). Naphthalene, a classical PAH with possible carcinogenicity, has drawn considerable concerns because of its high water solubility and high volatility (Valdman et al. 2004b). As one of the most widespread xenobiotic pollutants, the detection and natural attenuation of naphthalene are the main challenges in PAH contamination (Valdman et al. 2004a).

Chemical analysis is the main approach for the detection of naphthalene in environmental samples. Despite their cost and laborious pre-treatment, gas chromatography/mass spectrometry (GC/MS) (Potter and Pawliszyn 1994) and high-performance liquid chromatography (Oliferova et al. 2005) are the most commonly applied techniques in environmental monitoring (Zhang et al. 2013). Recently, the increasing attention on genetically engineered whole-cell bioreporters attributed to their high sensitivity, low cost, time efficiency, and ease of operation (Song et al. 2009). More importantly, whole-cell bioreporters can assess the bioavailability and toxicity of contaminants in their natural environments (Deepthike et al. 2009, Kohlmeier et al. 2008, Tecon et al. 2009). They could further be used for *in situ* or online measurement of contaminants and evaluation of their ecological impacts (Chen et al. 2013, Elad et al. 2011). Whole-cell bioreporters are viewed as supplementary techniques to chemical analysis for environmental risk assessment. Numerous whole-cell bioreporters have been reported to sense crude oil and PAHs,

such as *n*-alkane (Zhang et al. 2012a), benzene, toluene, ethylbenzene, and xylene (Keane et al. 2008, Kuncova et al. 2011), naphthalene (King et al. 1990, Trogl et al. 2012), and phenanthrene (Shin et al. 2011) (Appendix 1). Particularly, for naphthalene, *Pseudomonas fluorescens* HK44 is the most commonly investigated naphthalene bioreporter (King et al. 1990, Trogl et al. 2007). *P. fluorescens* HK44 can not only be directly applied in wastewater monitoring (Valdman et al. 2004b) but can also achieve online naphthalene detection (Valdman et al. 2004a), PAH degradation assessment (Paton et al. 2009), or immobilized in gel to retain its long storage time (Trogl et al. 2005). The bacterial biosensor HK44 has been shown to respond to sensitively and quantitatively to naphthlene (Paton et al. 2009). Indeed, while the biosensor in the study of polar organic contaminants in soil has been reported, their application in soil is less common(Semple et al. 2003). Currently, the biosensors need to interface with such target pollutants either following a suitable organic solvent extraction step or pioneering a technique directly via the gas phase(Heitzer et al. 1994). Most biosensor of naphthalene applications have remained in research lab for many reasons, some of which relate to a lack of standardization, the difficulty in maintaining living microbes, and also the poor analytical quality of the assays, poor specificities of detection, and the high detection limits(Werlen et al. 2004b).

Nevertheless, many other types of PAHs are still undetectable by living organisms. The fusing of reporter genes to the promoters of degradation genes and the use of biological signaling chains coupled to fluorescent or bioluminescent proteins are attributed to the construction principle (Belkin 2003, van der Meer et al. 2004). For instance, the conventional methods for naphthalene bioreporter construction followed the fusion of *lux* or *gfp* reporter gene in the operon (like *nahR*) encoding naphthalene metabolism (Shin 2010), hosted by indigenous naphthalene-degrading microbes (e.g.,

P. fluorescens) (King et al. 1990) or genetically engineered model strains (e.g., *Escherichia coli*) (Mitchell and Gu 2005), thereby allowing the expression of biological signals during naphthalene degradation (Ripp et al. 2000). The construction of each bioreporter is unique and laborious for specific PAH molecules. Most PAH metabolism occurs via the salicylate pathway, including naphthalene (Chen and Aitken 1999, Harwood and Parales 1996, Johri et al. 1999, Loh and Yu 2000, Yen and Serdar 1988), and salicylate behaved as a significant signaling metabolite for whole-cell bioreporters. By cloning naphthalene-degrading operons into the salicylate bioreporter host, whole-cell bioreporters detect metabolic salicylate and quantify the existence of the parent naphthalene in natural environment. This technique is also applied for the construction of series PAHs whole-cell bioreporters for multi sensing array.

In this study, a new type of naphthalene bioreporter was constructed and applied in groundwater and soil naphthalene contamination measurement. A Gibson isothermal assembly (Gibson et al. 2009) was introduced for the construction of a recombinant naphthalene-degrading plasmids, pWH1274_Nah, with the capability of transferring naphthalene to the central metabolite salicylate. The new bioreporter, ADPWH_Nah, was constructed by cloning the pWH1274_Nah vector in the host *Acinetobacter* ADPWH_lux (Huang et al. 2005) and the *salAR* and *luxCDABE* operons, which were inducible by salicylate. Converting naphthalene to salicylate by the expression of *nahAD* operon on the vector, the ADPWH_Nah bioreporter was able to quantitatively respond to naphthalene and assess naphthalene contamination in natural water and soil. The naphthalene-degrading pWH1274_Nah vector could be replaced by other plasmids with respective PAH metabolic operons to achieve the biological detection of targeting PAHs. Our work presented a routine and simple method for the

116 construction of various bioreporters responsive to different PAH molecules, exhibiting
117 its extensive application possibilities in water and soil monitoring and assessment.

118 2. Materials and methods

119 *2.1 Bacterial strains, plasmids, and culture media*

120 The bacterial strains and plasmids are listed in **Table 1**. Unless otherwise stated, all
121 the chemicals are analytical-grade reagents. Luria–Bertani (LB) was used as the
122 cultivation medium for ADPWH_lux (Thermo Scientific, USA). ADPWH_Nah and
123 ADPWH_1274 were cultivated and induced in LB medium supplemented with 300
124 μg/mL ampicillin (LBA300); *E. coli* DH5α (with pWH1274 or pWH1274_NaAD)
125 was also cultivated in LBA300 medium. Minimal medium with 20 mM sodium
126 succinate (MMS) was used for the induction of bioreporter strains, containing 2.5 g
127 Na_2HPO_4, 2.5 g KH_2PO_4, 1.0 g NH_4Cl, 0.1 g $MgSO_4 \cdot 7H_2O$, 10 μL saturated $CaCl_2$
128 (44.8%), 10 μL saturated $FeSO_4$ (20.8%), 1 mL Bauchop and Elsden solution, and 20
129 mM sodium succinate in 1.0 L deionized water. Minimal medium agar (1.4%, MMA)
130 was supplemented with naphthalene crystals as the sole carbon source for the
131 selection of positive *Acinetobacter* clone with pWH1274_Nah vector.

132 *2.2 Gibson isothermal assembly for pWH1274_Nah plasmid construction*

133 The Gibson cloning and construction of naphthalene whole-cell bioreporter
134 ADPWH_Nah is briefly illustrated in **Fig. 1**. Our targeting vector, pWH1274_ Nah,
135 was assembled by the *nahAD* operon (9 kb, **Fig. 1A**) and pWH1274 plasmid (6 kb,
136 **Fig. 1A**), with the one-step *in vitro* Gibson recombination method which can
137 assemble DNA products as large as 900 kb (Gibson et al. 2009). pDTG1 plasmids
138 (Dennis and Zylstra 2004) were extracted from *Pseudomonas putida* NCIB9816
139 (Cane and Williams 1982) as the template for the *nahAD* operon. The primers

(Sangon Biotech, China) for polymerase chain reaction (PCR) and Gibson isothermal assembly are listed in **Table 2**. The two pairs of primers were designed and synthesized with a 30+ bp overlap (**Fig. 1B**). pWH1274 and *nahAD* operons were separately amplified by PCR using the primer pairs NahA_for/NahD_rev and 1274_for/1274_rev (**Table 2**). The PCR system (50 μL) contained 1 μL DNA template, 1× reaction buffer, 0.2 mM each of deoxynucleoside triphosphate (Fermentas, USA), 0.2 μM each of primer, and 2.5 units Dream Taq DNA polymerase (Fermentas, USA). The reaction was performed with initial denaturation at 95 °C for 4 min, followed by 35 cycles of 95 °C for 30 s, 56 °C for 30 s, and 72 °C for 5 min, and a final additional extension at 72 °C for 10 min. The amplified products were isolated from 1% agarose gel and further purified with QIAquick gel extraction kit (Qiagen, Germany) according to the manufacturer's instructions. The two fragments were processed and fused together using a T5 exonuclease, TaqDNA ligase, and high-fidelity Phusion polymerase, incubated at 50 °C for 12 h (**Fig. 1B**). After transformation via heat shock, the positive clone (DH5α_pWH1274_Nah) was selected on LBA300 agar plate and the plasmid pWH1274_Nah was extracted from DH5α_pWH1274_Nah cells.

2.3 Transformation of pWH1274 and pWH1274_Nah vector in ADPWH_lux

The competent cells of ADPWH_lux were prepared as the following: after growing in LB medium at 30 °C overnight with shaking at 150 rpm, the 100 μL cell suspension was harvested by centrifugation at 3000 rpm for 10 min at 4 °C, washed, and resuspended in 1 mL 10% glycerol. The 1 μL aliquot of the pWH1274_Nah or pWH1274 was electro-transformed into 50 μL competent ADPWH_lux cells. Subsequently, the cells were transferred into 500 μL of SOC medium and incubated at 30 °C for 2 h. The cell suspension was then spread on MMA with naphthalene crystals

for the selection of positive transformants capable of metabolizing naphthalene. The plasmid pWH1274 was also electro-transformed into *Acinetobacter* ADPWH_lux as the negative control with a similar selection process mentioned above, except for the LBA300 agar plate for selection. The confirmation of successful pWH1274_Nah vector transformation and function was verified by the metabolism of naphthalene and PCR amplification with NahA_for/NahD_rev primer pairs.

2.4 Bioluminescence induction of ADPWH_Nah by PAHs

Each of the 100 mM PAH and interfering substances stock solutions were prepared by dissolving a specific weight (naphthalene 128.2 mg, pyrene 202.3 mg, toluene 92.1 mg, anthracene 178.2 mg, phenanthrene 178.2 mg, sodium salicylate 160.1 mg, and sodium benzoate 144.1 mg) in 10 mL dimethyl sulfoxide (DMSO, for naphthalene, pyrene, toluene, anthracene, and phenanthrene) or deionized water (for sodium salicylate and sodium benzoate). The PAH and interfering substances induction solution was made by series dilution to the final concentration of 0, 1, 5, 10, 20, 50, and 100 μM with deionized water. After inoculation in LBA300 medium at 30 °C overnight, 1 mL ADPWH_Nah, ADPWH_1274, and ADPWH_lux cell suspensions were harvested by centrifugation at 3000 rpm for 10 min at 4 °C, washed twice, and resuspended in MMS medium of the same volume (Zhang et al. 2013). A 20 μL bioreporter suspension and a 180 μL PAH solution were transferred into each well of a 96-well black optical-flat microplate (Corning Costa, USA). The bioluminescence and absorbance at 600 nm wavelength (OD_{600}) of the microplate wells were detected by the Synergy 2 Multi-Detection Microplate Reader (BioTek Instrument, USA). The measurement was conducted every 10 min for 5 h and the incubation temperature was 30 °C. All detections were carried out in triplicates.

2.5 Naphthalene detection in PAHs-contaminated sites

A total of 16 real groundwater samples and 13 soil samples were collected from a PAHs-contaminated site in China (**Fig. 2**, and the locations are listed in **Table A1** and **Table A2** of Supplementary Material) on 14 July 2014. The site was historically contaminated by chemical spills from *China Petroleum Lanzhou Petrochemical Company*, consequently causing the *Lanzhou Tap Water Crisis* on 11 April 2014. Ten shallow groundwater samples (SW01, SW03, SW04, SW05, SW06, SW07, SW08, SW09, SW11, and SW15) were taken at 4.5 m depth, and the other six deep groundwater samples (DW02, DW05, DW07, DW08, DW09, and DW11) were collected at 8.0 m depth. Thirteen soil samples (a, b, c, d, e, f, g, h, i, j, k, l, m) were taken at three depths (0.5, 1.5, and 3 m). The samples were stored at 4 °C until further assessment (within 72 h). The chemical analysis of PAHs and *n*-alkane contamination was conducted by GC/MS following US EPA methods (Zhang et al. 2013), and the results are listed in **Tables A3 and A4**. A 2 mL groundwater sample was homogenized with 40 kHz ultrasound for 300 s and mixed well by vortexing for 10 s before bioreporter detection. A 360 mg soil sample mixed with 5 mL deionized water was homogenized with 40 kHz ultrasound for 300 s and vortexed for 10 s before bioreporter detection (Zhang et al. 2012a). The ADPWH_Nah bioreporter strains were cultivated in LB medium overnight at 30 °C, followed by centrifugation harvest (3000 rpm for 10 min), and resuspended in MMS medium. A 20 μL bioreporter suspension and a 180 μL groundwater sample/the supernatant of the soil solution were transferred into a 96-well black optical-flat microplate, following the same procedure for naphthalene solution detection above.

2.6 Quantitative model for ADPWH_Nah's response to naphthalene

From the mathematical gene regulation model for the bioreporter response to specfic chemicals (Al-Anizi et al. 2014, Zhang et al. 2012b), the direct induction of *salAR* operon in ADPWH_lux by salicylate can be expressed by the following equation.

$$\alpha_{[S]} = \alpha_{m[0]} + \alpha_m \cdot \frac{[S]}{K_I^{-1}+[S]} \quad (1)$$

Here, $[S]$ represents the salicylate concentration in bioreporter cells (cell^{-1}) and K_I refers to the specific inducer binding rate of the *SalR* regulon to the salicylate molecule. $\alpha_{m[0]}$ ($s^{-1}\cdot cell^{-1}$) is the transcription rate of the *salAR* operon baseline expression in the absence of the inducer, and α_m represents the maximal transcription rate with saturated salicylate induction. Considering the metabolization rate from naphthalene to salicylate (m_{N-S}) by NahAD enzymes, the researchers found that the salicylate concentration was the formula of naphthalene concentration ($[N]$, cell^{-1}), and Equation (2) then described the quantitative gene expression of the *salAR* operon induced by naphthalene.

$$\alpha_{[N]} = \alpha_{m[0]} + \alpha_m \cdot \frac{[N]}{(m_{N-S}\cdot K_I)^{-1}+[N]} \quad (2)$$

2.7 Data analysis

The distribution of naphthalene in groundwater and soil samples were interpolated by Kriging method, analyzed, and plotted by Surfer 8.0 (Golden Software). The SPSS package (version 11.0) was used for statistical analysis, and a p value<0.05 was considered to indicate statistical significance. The Brown–Forsythe and Shapiro–Wilk tests were performed for data equality and normality, and the null hypothesis was rejected for p values less than 0.05.

3. Results and discussions

3.1 Genetic information of naphthalene bioreporter ADPWH_Nah

Plasmid pWH1274 is a commonly used shuttle vector for *E. coli* and *Acinetobacter calcoaceticus* (Hunger et al. 1990). The *nahAD* operon encoding naphthalene metabolism was amplified by PCR from the pDTG1 plasmid in *Pseudomonas putida* NCIB9816 (**Table 1**) (Cane and Williams 1982). To improve the naphthalene metabolization to salicylate, the *nahAD* was cloned into pWH1274 with the constitutive promoter P_{tet} (Hansen and Sorensen 2000) via the Gibson isothermal assembly (Gibson et al. 2009) (**Fig. 1**). The pWH1274 and pWH1274_Nah vectors were then integrated into the salicylate bioreporter, ADPWH_lux, as the negative control (ADPWH_1274) and positive bioreporter strain (ADPWH_Nah) for naphthalene sensing.

The existence of nahAD operon in ADPWH_Nah was confirmed by PCR with the primer pairs NahD_rev/NahA_for (**Table 2**), and the results were negative for ADPWH_lux and ADPWH_1274 (Fig. A1). The PCR product had been sequenced to verify by the Illumina HiSeq and MiSeq platforms. ADPWH_Nah can grow on mineral medium supplemented with naphthalene as the sole source of carbon and energy, during which naphthalene is metabolized to salicylate by NahAD enzymes. The salicylate molecules further activated the Psal promoter and triggered the expression of salAR operon and luxCDABE gene, exhibiting bioluminescent signals for the detection. The new bioreporter ADPWH_Nah was constructed through the introduction of cloning pWH1274_Nah vector into host Acinetobacter ADPWH_lux. The bioluminescent bioreporter was functional when the vector converted naphthalene to salicylate and visible signaling mediated by the metabolite salicylate

was observed.

3.2 Naphthalene induction kinetics of ADPWH_Nah

In the absence of naphthalene, ADPWH_Nah, ADPWH_1274, and ADPWH_lux had a similar bioluminescent baseline from 50 RLU to 200 RLU (**Fig. 3A**). Exposed to 50 μM naphthalene, only ADPWH_Nah showed rapid positive response within 5 min, and the dramatic increasing bioluminescence lasted for 2 h and subsequently maintained a high level of 2500 RLU to 3100 RLU (**Fig. 3A**). No response was observed for ADPWH_1274 and ADPWH_lux to naphthalene, indicating that naphthalene did not activate the *salAR* operon and *luxCDABE* gene. The results proved the functions of *nahAD* operon for naphthalene metabolism, and P_{tet} was a strong promoter for *nahAD* expression and encoding compared with the *nahR* regulator (Mitchell and Gu 2005).

From the response of ADPWH_Nah to different naphthalene concentrations (**Fig. 3B**), the detection limit of ADPWH_Nah was 0.01 μM, and the quantification time was 1 h. The 5 μM naphthalene induction was significantly higher than the negative control within only 5 min after induction. The rapid and sensitive response of ADPWH_Nah suggested its potential in a real-time naphthalene whole-cell bioreporter. Throughout the induction, no significant growth suppression was observed (**Fig. A2**), indicating limited impacts of naphthalene on the growth and activities of ADPWH_Nah bioreporter. The increasing bioluminescence signal occurred in the first 2 h and the stable response time was identified from 200 min to 240 min. The positive relationship between ADPWH_Nah's bioluminescence and naphthalene concentration also indicated that ADPWH_Nah can be utilized to detect naphthalene in the aqueous phase.

ADPWH_Nah was found with high response specificity towards naphthalene, as illustrated in **Fig. 4**. With similar responsive pattern to sodium salicylate and sodium benzoate, the three strains had the same mechanisms of *salAR* operon activation by salicylate or benzoate (Zhang et al. 2012b). In the presence of different concentrations of pyrene, toluene, anthracene, and phenanthrene, ADPWH_Nah did not exhibit a significant response. With the response of the negative control ADPWH_1274 to salicylate and benzoate (**Fig. A3**), their disturbance can be mitigated.

3.2 The quantitative response of ADPWH_Nah to naphthalene

Fig. 5 further illustrates the quantitative response of ADPWH_Nah to different concentrations of naphthalene, sodium salicylate, and sodium benzoate. From the average bioluminescence response ratio between 200 and 240 min (stable response period), the mathematical model successfully predicted the behavior of ADPWH_Nah and the calculation fit well with the experimental data. The linear relationship between bioluminescent response and naphthalene was revealed when naphthalene concentration ranged from 1 μM to 50 μM. At higher concentration, the bioluminescent intensity became saturated, whereas the response ratio of ADPWH_Nah kept increasing for salicylate. This phenomenon was explained by the limited capacities of the *nahAD* to metabolize naphthalene into salicylate at high concentration.

Compared with the response of ADPWH_lux to various PAHs (Zhang et al. 2012b), the inductive ADPWH_Nah follows a similar gene expression rate and specific inducer binding rate ($s^{-1}\cdot cell^{-1}$), as listed in **Table 3**. The gene expression rate of ADPWH_Nah for napthlene was 130.4 $s^{-1}\cdot cell^{-1}$, similar to that of ADPWH_lux to salicylate (124.2 $s^{-1}\cdot cell^{-1}$), indicating the same promoter activation of *salAR* operon

and *luxCDABE* gene. The specific inducer binding rate K_I of ADPWH_Nah was 4310 $s^{-1}\cdot cell^{-1}$, significantly lower than 23,255 $s^{-1}\cdot cell^{-1}$ (the binding rate of salicylate to *salR* regulon in ADPWH_lux). The α_m of ADPWH_Nah's response to naphthalene was 53.2 $s^{-1}\cdot cell^{-1}$, much lower than that of ADPWH_Nah's response to salicylate, whereas its naphthalene K_I (75,301 $s^{-1}\cdot cell^{-1}$) was significantly higher than the value in salicylate induction (5181 $s^{-1}\cdot cell^{-1}$). The results suggested that the insufficient metabolization rate from naphthalene to salicylate (m_{N-S}, 0.069 from calculation), consequently resulted in low available salicylate to promote the *salAR* operon. ADPWH_Nah and ADPWH_lux had similar gene expression rates (46.4 $s^{-1}\cdot cell^{-1}$and 40.4 $s^{-1}\cdot cell^{-1}$respectively) and specific inducer binding rates (745 $s^{-1}\cdot cell^{-1}$ and 632 $s^{-1}\cdot cell^{-1}$, respectively), further confirming that the expression of *benM* operon in ADPWH_Nah was stimulated by salicylate, not benzoate, as in ADPWH_lux. It was the direct evidence for the *nahAD* encoding naphthalene metabolic pathway via salicylate instead of benzoate.

3.3 The response ofADPWH_Nahto PAHs-contaminated site

The distribution of naphthalene in the real PAHs-contaminated groundwater and soil samples, via both bioreporter and GC/MS analysis, demonstrated the reliability and feasibility of whole-cell bioreporter ADPWH_Nah in environmental monitoring and bioavailability assessment. With the response of the negative control ADPWH_1274 in groundwater and soil samples (**Fig. A4**), their disturbance can be mitigated.

At a groundwater depth of 4.5 m, significant total naphthalene concentration ranged from 6.0 μg/L to 63.4 μg/L (**Fig. 6B**). The highest total naphthalene contamination was found at SW07 (63.0 μg/L) and SW03 (42.3 μg/L). As for bioreporter-estimated naphthalene (**Fig. 6A**), SW03 had the highest contamination (64.0 μg/L), whereas

SW07 had an extremely low level of bioreporter-estimated naphthalene (3.0 μg/L). Given that SW03 was the latest contaminated point where the tap water contamination was found, it is proposed that the majority of PAHs were bioavailable after recent contamination. For SW07 with long contamination history, the bioavailable fraction of PAHs was metabolized by indigenous microbes, and low bioreporter-estimated naphthalene was found. At a depth of 8.0 m, similar spatial distribution of naphthalene contaminants was identified (**Fig. 6**). The highest bioreporter-estimated naphthalene and total naphthalene (33.0 and 66.5 μg/L, respectively) was observed at DW08, indicating the vertical transportation of PAHs contaminants from surface soil (SW08) to deeper soil (DW08) after long-term chemical spills. A positive relationship (Pearson coefficient was 0.548 and p value<0.01) was found between the bioreporter-estimated naphthalene (bioreporter data) and total naphthalene in groundwater (GC/MS data). ADPWH_1274 (6 h) in groundwater samples had a dynamic growth curve. No significant growth suppression was observed throughout the measurement, indicating limited impacts of naphthalene on the growth and activities of ADPWH_1274.

At a soil depth of 0.5 m, total naphthalene concentration ranged from 0.3 mg/kg to 12.4 mg/kg **(Fig. 6D)**. The highest bioreporter-estimated naphthalene and total naphthalene (8.86 and 12.4 mg/kg, respectively) was observed at point g. However, an extremely low level of bioreporter-estimated naphthalene was found in point j (0 mg/kg) (**Fig. 6C**). Since point g was the latest contaminated point, it is proposed that the majority of PAHs were bioavailable after recent contamination. For point j, with long contamination history, the bioavailable fraction of PAHs was metabolized by indigenous microbes. At depths of 1.5 and 3 m, similar spatial distribution of naphthalene contaminants was identified (**Fig. 6**). A positive relationship (Pearson

354 coefficient was 0.740 and *p* value<0.01) was found between the bioreporter-estimated
355 naphthalene (bioreporter data) and total naphthalene in soil (GC/MS data).

356 The results suggested that biological monitoring via whole-cell bioreporter
357 (ADPWH_Nah) was comparable to chemical analysis. More interestingly, the
358 (bioreporter-estimated)-to-total ratio gave more information on the chemical spill
359 history of the contaminated sites. The latest contaminated point SW03 in groundwater
360 had high (bioreporter-estimated)-to-total ratio of naphthalene (100%), and an
361 extremely low level of the ratio was found in SW07 with long contamination history
362 (4.4%). Accordingly, the recent contamination point g in soil had high bioavailable
363 fraction of the organic pollutants ((bioreporter-estimated)-to-total ratio is 71.5%),
364 suitable for bioremediation. Oppositely, the PAHs at the sites with long contamination
365 history, such as point j in soil ((bioreporter-estimated)-to-total ratio is 30.2%), had
366 low bioavailability, and chemical/physical remediation approaches were suggested.
367 Overall, the average (bioreporter-estimated)-to-total ratio of naphthalene in
368 groundwater is 74.8%, similar to that in soil (67.8%), indicating that both the
369 groundwater and soil were from the same source as the historical oil spills. Although
370 the ratio was a little higher in groundwater, it may be because more hydrophilic
371 organic matters moved to groundwater while high molecular hydrophobic matters
372 were retained in the soil. Given the rapid detection time (less than 6 h) and low
373 sample volume requirement (180 μL), the whole-cell bioreporter is a supplementary
374 tool for environmental assessment decision making and site management.

375 ### *3.4 Multi whole-cell bioreporter array for high-throughput PAHs assessment*

376 A multi whole-cell bioreporter array has been applied for hydrocarbons (Tecon et al.
377 2010); however, no such high-throughput PAH bioreporter array exists. From the

conventional approach of bioreporter construction, the laborious and unique cloning work for the specific PAHs molecule is not suitable for the routine approaches. The performance of different bioreporter strains was also affected by respective environmental factors, such as carbon source or temperature, and the whole-cell bioreporter array therefore suffers from calibration and standardization variations. With the salicylate bioreporter ADPWH_lux, the clone of ring-hydroxylating dioxygenase genes (Cebron et al. 2008) with stronger-expressed promoter helps in the assembly of a multi whole-cell bioreporter array for various PAH molecules. The *phnAaBAcAdDHGCF* operon from *Acidovorax* NA3 (Singleton et al. 2009) was capable of metabolizing phenanthrene via the salicylate pathway (Pinyakong et al. 2000). To achieve online and high sensitivity, the choice of reporter gene was important, and *lacZ*, *gfp*, and *lux* reporter genes have their respective advantages and challenges (Kohlmeier et al. 2007). Other *nidDBAC* in *Mycobacterium vanbaalenii* PYR-1 (Kim et al. 2006) was also responsible for pyrene and mineralization, viewed as the candidate for the corresponding circuit component for the whole-cell bioreporter. By mining the new functional genes (Wang et al. 2010), more metabolic building blocks could be characterized and more specific whole-cell bioreporter would be arrayed, based on the salicylate metabolite pathway and response, for high-throughput PAH detection.

4. Conclusions

This study developed a new whole-cell bioreporter, ADPWH_Nah, for the rapid detection of naphthalene in environmental samples. The bioreporter has high specificity to sense naphthalene and successfully evaluates the spatial distribution of naphthalene in groundwater after the *Lanzhou Tap Water Crisis*. The findings also

suggest it is possible for multiple PAHs whole-cell bioreporter construction, metabolizing PAHs by introducing a functional operon into a sensible salicylate to assemble a bioreporter array for rapid and high-throughput environmental monitoring.

Acknowledgement

This work was supported by National Natural Science Foundation of China (51178048, 51378064 and 41301331).

5. References

Al-Anizi, A.A., Hellyer, M.T. and Zhang, D. (2014) Toxicity assessment and modeling of *Moringa oleifera* seeds in water purification by whole cell bioreporter. Water Research 56, 77-87.

Belkin, S. (2003) Microbial whole-cell sensing systems of environmental pollutants. Current Opinion in Microbiology 6(3), 206-212.

Boffetta, P., Jourenkova, N. and Gustavsson, P. (1997) Cancer risk from occupational and environmental exposure to polycyclic aromatic hydrocarbons. Cancer Causes and Control 8(3), 444-472.

Cane, P.A. and Williams, P.A. (1982) The plasmid-coded metabolism of naphthalene and 2-methylnaphthalene in *Pseudomonas* strains, phenotypic changes correlated with structural modification of the plasmid pWW60-1. Journal of General Microbiology 128(OCT), 2281-2290.

Cebron, A., Norini, M.-P., Beguiristain, T. and Leyval, C. (2008) Real-Time PCR quantification of PAH-ring hydroxylating dioxygenase (PAH-RHD alpha) genes from Gram positive and Gram negative bacteria in soil and sediment samples. Journal of Microbiological Methods 73(2), 148-159.

Chen, C., Zhang, D., Thornton, S.F., Duan, M., Luo, Y., Ding, A. and Huang, W.E. (2013) Functionalization and immobilization of whole cell bioreporters for the detection of environmental contamination. Environmental Engineering and Management Journal 12(7), 1417-1422.

Chen, S.H. and Aitken, M.D. (1999) Salicylate stimulates the degradation of high molecular weight polycyclic aromatic hydrocarbons by *Pseudomonas saccharophila* P15. Environmental Science & Technology 33(3), 435-439.

Cho, J.H., Lee, D.Y., Lim, W.K. and Shin, H.J. (2014) A recombinant Escherichia coli biosensor for detectiong polycyclic aromatic hydrocarbons in gas and aqueous phases. Preparative Biochemistry and Biotechnology 44(8), 849-860.

Deepthike, H.U., Tecon, R., van Kooten, G., van der Meer, J.R., Harms, H., Wells, M. and Short, J. (2009) Unlike PAHs from Exxon Valdez Crude Oil, PAHs from Gulf of Alaska Coals are not Readily Bioavailable. Environmental Science & Technology 43(15), 5864-5870.

Dennis, J.J. and Zylstra, G.J. (2004) Complete sequence and genetic organization of pDTG1, the 83 kilobase naphthalene degradation plasmid from *Pseudomonas putida* strain NCIB 9816-4. Journal of Molecular Biology 341(3), 753-768.

Elad, T., Almog, R., Yagur-Kroll, S., Levkov, K., Melamed, S., Shacham-Diamand, Y. and Belkin, S. (2011) Online Monitoring of Water Toxicity by Use of Bioluminescent Reporter Bacterial Biochips. Environmental Science & Technology 45(19), 8536-8544.

Gibson, D.G., Young, L., Chuang, R.-Y., Venter, J.C., Hutchison, C.A., III and Smith, H.O. (2009) Enzymatic assembly of DNA molecules up to several hundred kilobases. Nature Methods 6(5), 343-U341.

Hansen, L.H. and Sorensen, S.J. (2000) Detection and quantification of tetracyclines by whole cell biosensors. FEMS Microbiology Letters 190(2), 273-278.

Harwood, C.S. and Parales, R.E. (1996) The beta-ketoadipate pathway and the biology of self-identity. Annual Review of Microbiology 50, 553-590.

Heitzer, A., Malachowsky, K., Thonnard, J.E., Bienkowski, P.R., White, D.C. and Sayler, G.S. (1994) Optical biosensor for environmental on-line monitoring of naphthalene and salicylate bioavailability with an immobilized bioluminescent catabolic reporter bacterium. Applied & Environmental Microbiology 60(5), 1487-1494.

Huang, W.E., Wang, H., Zheng, H.J., Huang, L.F., Singer, A.C., Thompson, I. and

Whiteley, A.S. (2005) Chromosomally located gene fusions constructed in *Acinetobacter sp* ADP1 for the detection of salicylate. Environmental Microbiology 7(9), 1339-1348.

Hunger, M., Schmucker, R., Kishan, V. and Hillen, W. (1990) Analysis and nucleotide sequence of an origin of DNA replication in *Acinetobacter-calcoaceticus* and its use for *Escherichia-coli* shuttle plasmids. Gene 87(1), 45-51.

Johri, A.K., Dua, M., Singh, A., Sethunathan, N. and Legge, R.L. (1999) Characterization and regulation of catabolic genes. Critical Reviews in Microbiology 25(4), 245-273.

Keane, A., Lau, P.C.K. and Ghoshal, S. (2008) Use of a whole-cell biosensor to assess the bioavailability enhancement of aromatic hydrocarbon compounds by nonionic surfactants. Biotechnology and Bioengineering 99(1), 86-98.

Kim, S.J., Kweon, O., Freeman, J.P., Jones, R.C., Adjei, M.D., Jhoo, J.W., Edmondson, R.D. and Cerniglia, C.E. (2006) Molecular cloning and expression of genes encoding a novel dioxygenase involved in low- and high-molecular-weight polycyclic aromatic hydrocarbon degradation in Mycobacterium vanbaalenii PYR-1. Applied and Environmental Microbiology 72(2), 1045-1054.

King, J.M.H., Digrazia, P.M., Applegate, B., Burlage, R., Sanseverino, J., Dunbar, P., Larimer, F. and Sayler, G.S. (1990) Rapid, sensitive bioluminescent reporter technology for naphthalene exposure and biodegradation. Science 249(4970), 778-781.

Kohlmeier, S., Mancuso, M., Deepthike, U., Tecon, R., van der Meer, J.R., Harms, H. and Wells, M. (2008) Comparison of naphthalene bioavailability determined by whole-cell biosensing and availability determined by extraction with Tenax. Environmental Pollution 156(3), 803-808.

Kohlmeier, S., Mancuso, M., Tecon, R., Harms, H., van der Meer, J.R. and Wells, M. (2007) Bioreporters: gfp versus lux revisited and single-cell response. Biosensors & Bioelectronics 22(8), 1578-1585.

Kuncova, G., Pazlarova, J., Hlavata, A., Ripp, S. and Sayler, G.S. (2011) Bioluminescent bioreporter Pseudomonas putida TVA8 as a detector of water

pollution. Operational conditions and selectivity of free cells sensor. Ecological Indicators 11(3), 882-887.

Loh, K.C. and Yu, Y.G. (2000) Kinetics of carbazole degradation by *Pseudomonas putida* in presence of sodium salicylate. Water Research 34(17), 4131-4138.

Mitchell, R.J. and Gu, M.B. (2005) Construction and evaluation of nagR-nagAa :: lux fusion strains in biosensing for salicylic acid derivatives. Applied Biochemistry and Biotechnology 120(3), 183-197.

Oliferova, L., Statkus, M., Tsysin, G., Shpigun, O. and Zolotov, Y. (2005) On-line solid-phase extraction and HPLC determination of polycyclic aromatic hydrocarbons in water using fluorocarbon polymer sorbents. Analytica Chimica Acta 538(1-2), 35-40.

Paton, G.I., Reid, B.J. and Semple, K.T. (2009) Application of a luminescence-based biosensor for assessing naphthalene biodegradation in soils from a manufactured gas plant. Environmental Pollution 157(5), 1643-1648.

Pinyakong, O., Habe, H., Supaka, N., Pinpanichkarn, P., Juntongjin, K., Yoshida, T., Furihata, K., Nojiri, H., Yamane, H. and Omori, T. (2000) Identification of novel metabolites in the degradation of phenanthrene by Sphingomonas sp strain P2. FEMS Microbiology Letters 191(1), 115-121.

Potter, D.W. and Pawliszyn, J. (1994) Rapid determination of polyaromatic hydrocarbons and polychlorinated biphenyls in water using solid-phase microextraction and GC/MS. Environmental Science & Technology 28(2), 298-305.

Ripp, S., Nivens, D.E., Ahn, Y., Werner, C., Jarrell, J., Easter, J.P., Cox, C.D., Burlage, R.S. and Sayler, G.S. (2000) Controlled field release of a bioluminescent genetically engineered microorganism for bioremediation process monitoring and control. Environmental Science & Technology 34(5), 846-853.

Semple, K.T., Morriss, A.W.J. and Paton, G.I. (2003) Bioavailability of hydrophobic organic contaminants in soils: fundamental concepts and techniques for analysis. European Journal of Soil Science 54(4), 809-818.

Shin, D., Moon, H.S., Lin, C.C., Barkay, T. and Nam, K. (2011) Use of reporter-gene based bacteria to quantify phenanthrene biodegradation and toxicity in soil.

519 Environmental Pollution 159(2), 509-514.
520 Shin, H.J. (2010) Development of highly-sensitive microbial biosensors by mutation
521 of the nahR regulatory gene. Journal of Biotechnology 150(2), 246-250.
522 Singleton, D.R., Ramirez, L.G. and Aitken, M.D. (2009) Characterization of a
523 Polycyclic Aromatic Hydrocarbon Degradation Gene Cluster in a
524 Phenanthrene-Degrading Acidovorax Strain. Applied and Environmental
525 Microbiology 75(9), 2613-2620.
526 Song, Y., Li, G., Thornton, S.F., Thompson, I.P., Banwart, S.A., Lerner, D.N. and
527 Huang, W.E. (2009) Optimization of Bacterial Whole Cell Bioreporters for Toxicity
528 Assay of Environmental Samples. Environmental Science & Technology 43(20),
529 7931-7938.
530 Tecon, R., Beggah, S., Czechowska, K., Sentchilo, V., Chronopoulou, P.-M.,
531 McGenity, T.J. and van der Meer, J.R. (2010) Development of a Multistrain Bacterial
532 Bioreporter Platform for the Monitoring of Hydrocarbon Contaminants in Marine
533 Environments. Environmental Science & Technology 44(3), 1049-1055.
534 Tecon, R., Binggeli, O. and van der Meer, J.R. (2009) Double-tagged fluorescent
535 bacterial bioreporter for the study of polycyclic aromatic hydrocarbon diffusion and
536 bioavailability. Environmental Microbiology 11(9), 2271-2283.
537 Trogl, J., Ripp, S., Kuncova, G., Sayler, G.S., Churava, A., Parik, P., Demnerova, K.,
538 Halova, J. and Kubicova, L. (2005) Selectivity of whole cell optical biosensor with
539 immobilized bioreporter Pseudomonas fluorescens HK44. Sensors and Actuators
540 B-Chemical 107(1), 98-103.
541 Trogl, J., Kuncova, G., Kubicova, L., Parik, P., Halova, J., Demnerova, K., Ripp, S.
542 and Sayler, G.S. (2007) Response of the bioluminescent bioreporter Pseudomonas
543 fluorescens HK44 to analogs of naphthalene and salicylic acid. Folia Microbiologica
544 52(1), 3-14.
545 Trogl, J., Chauhan, A., Ripp, S., Layton, A.C., Kuncova, G. and Sayler, G.S. (2012)
546 *Pseudomonas fluorescens* HK44: Lessons Learned from a Model Whole-Cell
547 Bioreporter with a Broad Application History. Sensors 12(2), 1544-1571.
548 Valdman, E., Valdman, B., Battaglini, F. and Leite, S.G.F. (2004a) On-line detection

549 of low naphthalene concentrations with a bioluminescent sensor. Process
550 Biochemistry (Amsterdam, Netherlands) 39(10), 1217-1222.
551 Valdman, E., Battaglini, F., Leite, S.G.F. and Valdman, B. (2004b) Naphthalene
552 detection by a bioluminescence sensor applied to wastewater samples. Sensors and
553 Actuators B-Chemical 103(1-2), 7-12.
554 van der Meer, J.R., Tropel, D. and Jaspers, M. (2004) Illuminating the detection chain
555 of bacterial bioreporters. Environmental Microbiology 6(10), 1005-1020.
556 Wang, Y., Zhang, D. and Huang, W.E. (2010) Synthetic biology approach for mining
557 new enzymes from unculturable microorganisms. Luminescence 25(2), 104-104.
558 Werlen, C., Jaspers, M.C. and van der Meer, J.R. (2004a) Measurement of
559 biologically available naphthalene in gas and aqueous phases by use of a
560 Pseudomonas putida biosensor. Applied and Environmental Microbiology 70(1),
561 43-51.
562 Werlen, C., Jaspers, M.C. and Jr, V.D.M. (2004b) Measurement of biologically
563 available naphthalene in gas and aqueous phases by use of a Pseudomonas putida
564 biosensor. Applied & Environmental Microbiology 70(1), 43-51.
565 Wilcke, W. (2000) Polycyclic aromatic hydrocarbons (PAHs) in soil - a review.
566 Journal of Plant Nutrition and Soil Science-Zeitschrift Fur Pflanzenernahrung Und
567 Bodenkunde 163(3), 229-248.
568 Yen, K.M. and Serdar, C.M. (1988) Genetics of naphthalene catabolism in
569 *Pseudomonads*. CRC Critical Reviews in Microbiology 15(3), 247-268.
570 Zhang, D., Zhao, Y., He, Y., Wang, Y., Zhao, Y., Zheng, Y., Wei, X., Zhang, L., Li,
571 Y., Jin, T., Wu, L., Wang, H., Davison, P.A., Xu, J. and Huang, W.E. (2012a)
572 Characterization and Modeling of Transcriptional Cross-Regulation in *Acinetobacter*
573 *baylyi* ADP1. Acs Synthetic Biology 1(7), 274-283.
574 Zhang, D., He, Y., Wang, Y., Wang, H., Wu, L., Aries, E. and Huang, W.E. (2012b)
575 Whole-cell bacterial bioreporter for actively searching and sensing of alkanes and oil
576 spills. Microbial Biotechnology 5(1), 87-97.
577 Zhang, D., Ding, A., Cui, S., Hu, C., Thornton, S.F., Dou, J., Sun, Y. and Huang, W.E.
578 (2013) Whole cell bioreporter application for rapid detection and evaluation of crude

579 oil spill in seawater caused by Dalian oil tank explosion. Water Research 47(3),
580 1191-1200.

581

582

Table

Table 1 Bacterial strains and plasmids used in this study.

Table 2. Primers used in this study.

Table 3. The model parameters of ADPWH_lux and ADPWH_Nah response to various PAHs.

Table 1 Bacterial strains and plasmids used in this study.

Strain/plasmid	Description	Reference
Bacteria		
Escherichia coli DH5α	High efficient competent cells.	Tiangen, China
Pseudomonas putida NCIB9816	Naphthalene degrader with NahAD operon (9 kb) for naphthalene metabolization.	(Cane and Williams 1982)
Escherichia coli DH5α_pWH1274_Nah	*Escherichia* cells with pWH1274_Nah vector.	This study
ADPWH_lux	*Acinetobacter* bioreporter responsive to salicylate. A promoterless *luxCDABE* from pSB417 was inserted between *salA* and *salR* genes in the chromosome of ADP1.	(Huang et al. 2005)
ADPWH_Nah	*Acinetobacter* bioreporter responsive to naphthalene. The pWH1274_Nah vector exited in ADPWH_lux.	This study
ADPWH_1274	*Acinetobacter* bioreporter as the negative control of ADPWH_Nah. The pWH1274 vector exited in ADPWH_lux.	This study
Plasmids		
pDTG1	Plasmid with the NahAD operon (9 kb) from *Pseudomonas putida* NCIB9816.	(Dennis and Zylstra 2004)
pWH1274	*Escherichia coli* and *Acinetobacter baylyi* shuttle plasmid (6 kb), containing P_{tet} constitutive promoter and *Eco*RV restriction site for cloning. Ampicillin is used as antibiotic selection.	(Hunger et al. 1990)
pWH1274_Nah	NahAD operon cloned into the *Eco*RV site of pWH1274 vector.	This study

Table 2. Primers used in this study.

Primers	**Sequence (5'→3')**
NahA_for	AGGCTTGGTTATGCCGGTACTGCCGGGCCTCTTGCG GGATATTGACATATAACGTCGTATTCACG
NahD_rev	GCACGCCATAGTGACTGGCGATGCTGTCGGAATGGA CGATACGATCAGGTCAACCACTTATATC
1274_for	ATCGTCCATTCCGACAGCATCGCC
1274_rev	ATCCCGCAAGAGGCCCGGCAGTAC

Table 3. The model parameters of ADPWH_lux and ADPWH_Nah response to various PAHs.

Inducer	Bioreporter strains			
	Gene expression rate ($s^{-1} \cdot cell^{-1}$)		Specific inducer binding rate K_I ($s^{-1} \cdot cell^{-1}$)	
	ADPWH_lux	ADPWH_Nah	ADPWH_lux	ADPWH_Nah
Salicylate	124.2	130.4	23255	5181
Naphthalene	-	53.2	-	75301
Benzoate	46.4	40.4	745	632

Figure

Fig. 1. Schematics of ADPWH_Nah construction and response mechanisms. (A) PCR amplification of pDTG1 (9 kb) for naphthalene-degrading operon *nahAD* and pWH1274 (6 kb) plasmid for transformation vector. (B) Gibson isothermal assembly for pWH1274_NaAD vector. (C) Naphthalene metabolism and the induction of *salAR* operon by central metabolite salicylate.

Fig. 2. Contaminated sites and sampling points. Lanzhou City is located in northwest China (A), and the contaminated site is in the west city area and near the Yellow River (B). Ten groundwater samples were collected at a 4.5 m depth (C), and six groundwater samples were collected at an 8.0 m depth (D). Thirteen soil samples were collected at 0.5, 1.5, and 3 m depths (E).

Fig. 3. (A) Dynamic bioluminescence response of ADPWH_Nah and ADPWH_1274 to naphthalene inducer. The relative bioluminescence response to negative control (DMSO-MMS) ranged from 50 RLU to 200 RLU for ADPWH_Nah, ADPWH_1274, and ADPWH_lux. In the presence of 50 μM naphthalene in DMSO-MMS, the highest bioluminescent signal of ADPWH_Nah was 3077±62 RLU, significantly higher than that of ADPWH_1274 (119±3 RLU) and ADPWH_lux (131±19 RLU). (B) Quantitative response of ADPWH_Nah to a series of naphthalene concentrations. Kinetic responsive curve of ADPWH_Nah in the presence of 0, 1, 5, 10, 20, 50, and 100 μM naphthalene.

Fig. 4. The response of ADPWH_Nah (A), ADPWH_1274 (B) and ADPWH_lux (C) to various PAHs and interfering substances. The three whole-cell bioreporters had the same responsive pattern to sodium salicylate and sodium benzoate, illustrating their

similar stimulation mechanisms of *salAR* operon activation by salicylate or benzoate. ADPWH_Nah exhibited the unique positive response to naphthalene, but no response in the presence of pyrene, toluene, anthracene, and phenanthrene.

Fig. 5. The model simulation of ADPWH_Nah's response to different concentrations of naphthalene (R^2=0.98, RMSE=3.38), sodium salicylate (R^2=1, RMSE=1.58), and sodium benzoate (R^2=1, RMSE=0.33). The experimental data were the average bioluminescence response ratios of ADPWH_Nah between 200 and 240 min induction.

Fig. 6. Naphthalene contamination in groundwater and soil. The bioreporter-estimated naphthalene in groundwater (μg/L) (A) and soil (mg/kg) (C) were analyzed by whole-cell bioreporter, and calculated from the model simulation. The total naphthalene in groundwater (μg/L) (B) and soil (mg/kg) (D) were obtained by GC/MS. The contaminant distribution was plotted by Surfer 8.0 (Golden Software). A positive relationship was found between bioreporter-estimated naphthalene and total naphthalene in groundwater (Pearson coefficient is 0.548 and p value<0.05), and soil (Pearson coefficient is 0.740 and p value<0.05).

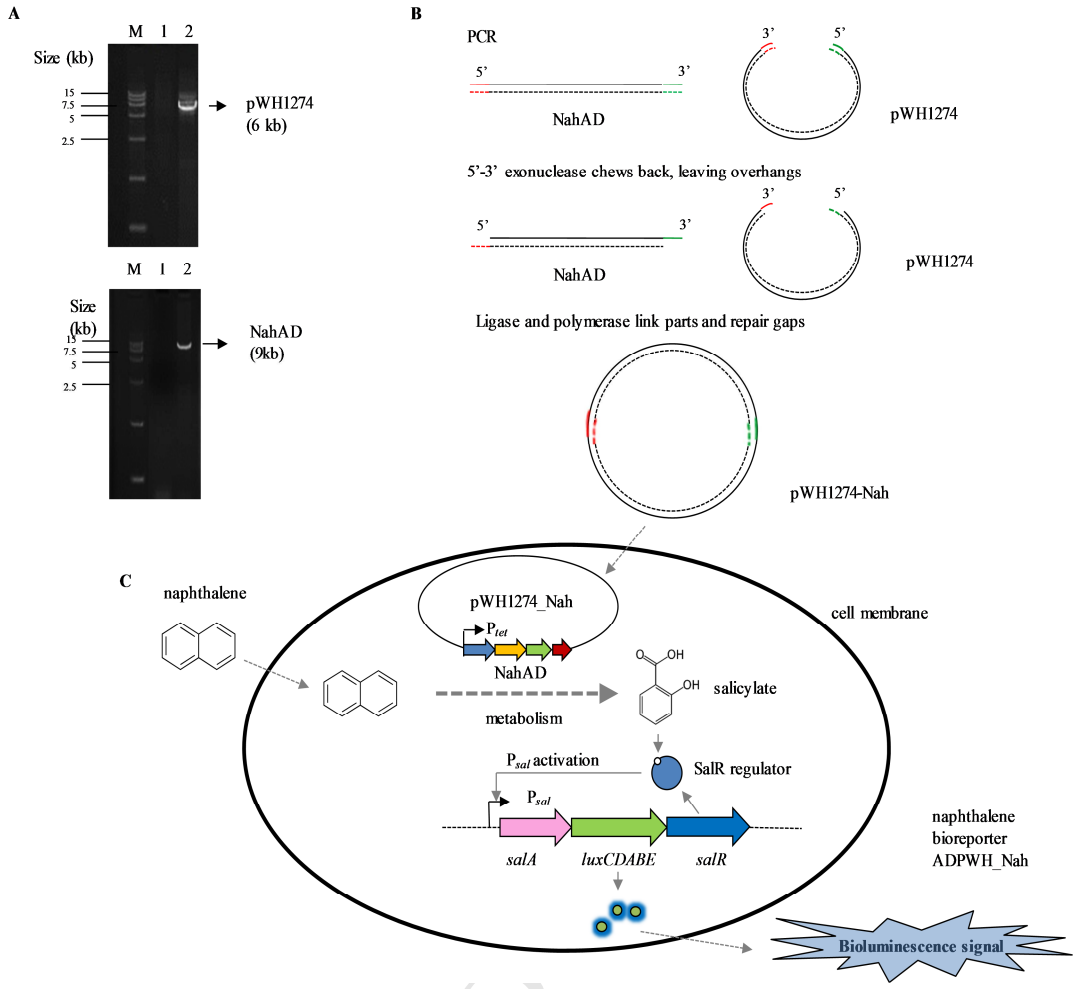

Fig. 1. Schematics of ADPWH_Nah construction and response mechanisms. (A) PCR amplification of pDTG1 (9 kb) for naphthalene-degrading operon *nahAD* and pWH1274 (6 kb) plasmid for transformation vector. (B) Gibson isothermal assembly for pWH1274_NaAD vector. (C) Naphthalene metabolism and the induction of *salAR* operon by central metabolite salicylate..

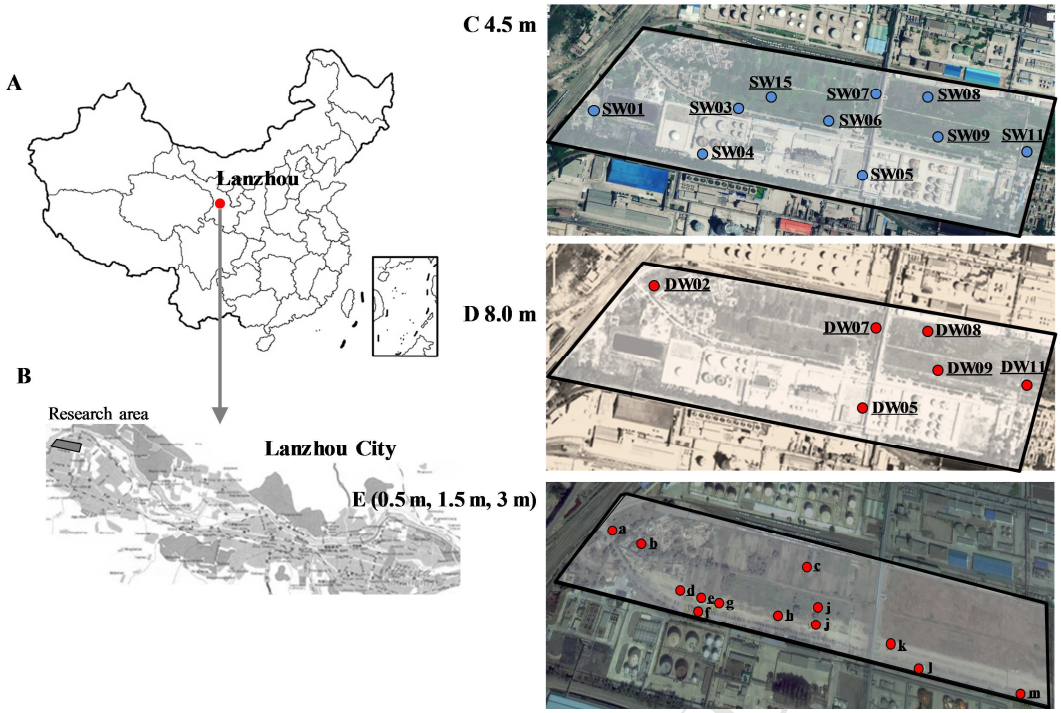

46

47 **Fig. 2.** Contaminated sites and sampling points. Lanzhou City is located in northwest
48 China (A), and the contaminated site is in the west city area and near the Yellow River
49 (B). Ten groundwater samples were collected at a 4.5 m depth (C), and six
50 groundwater samples were collected at an 8.0 m depth (D). Thirteen soil samples
51 were collected at 0.5, 1.5, and 3 m depths (E).

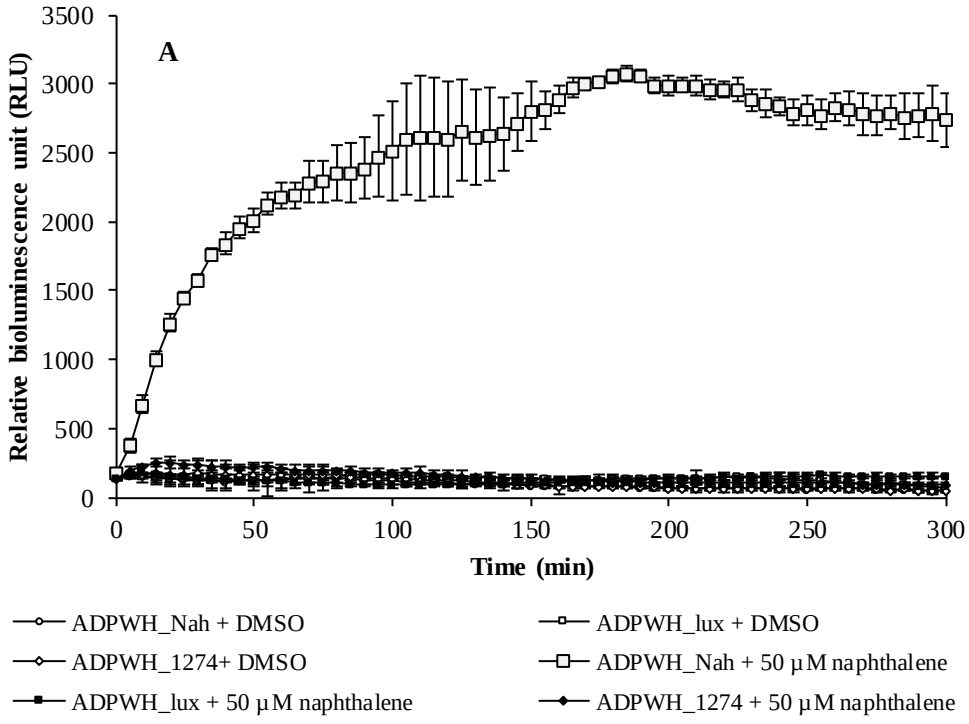

52

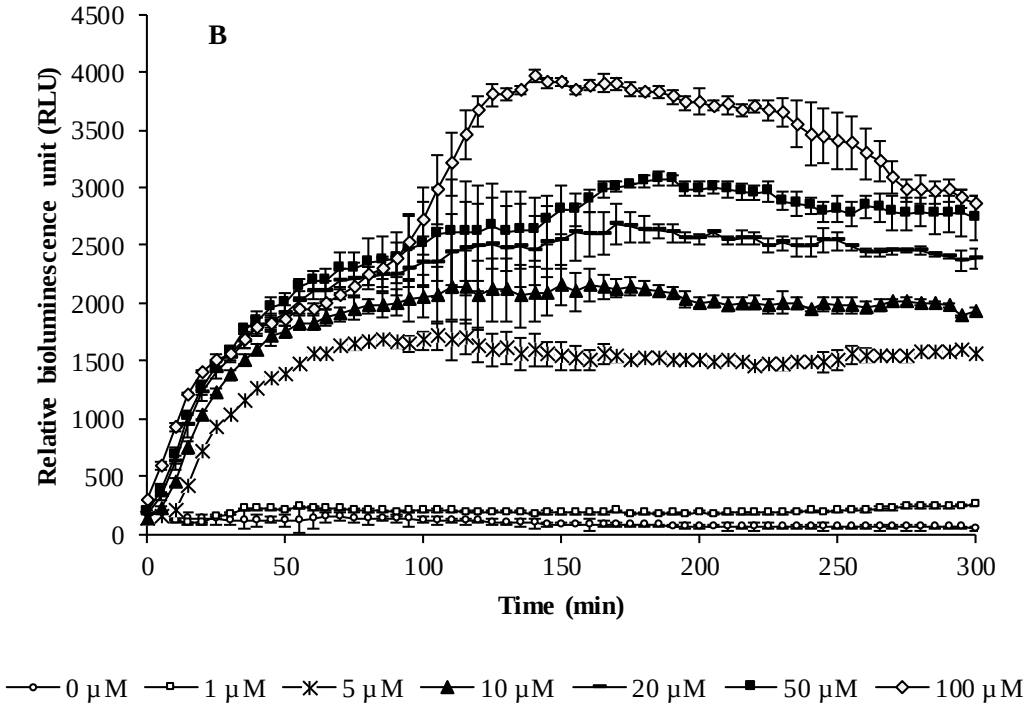

53

54 **Fig. 3.** (A) Dynamic bioluminescence response of ADPWH_Nah and ADPWH_1274
55 to naphthalene inducer. The relative bioluminescence response to negative control
56 (DMSO-MMS) ranged from 50 RLU to 200 RLU for ADPWH_Nah, ADPWH_1274,
57 and ADPWH_lux. In the presence of 50 µM naphthalene in DMSO-MMS, the highest

bioluminescent signal of ADPWH_Nah was 3077±62 RLU, significantly higher than that of ADPWH_1274 (119±3 RLU) and ADPWH_lux (131±19 RLU). (B) Quantitative response of ADPWH_Nah to a series of naphthalene concentrations. Kinetic responsive curve of ADPWH_Nah in the presence of 0, 1, 5, 10, 20, 50, and 100 μM naphthalene.

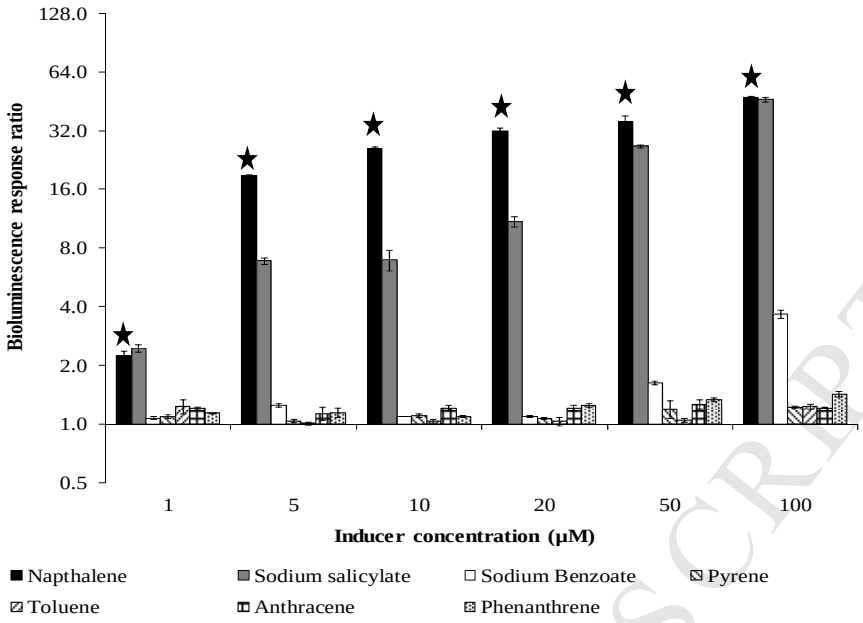

63

64 **(A)**

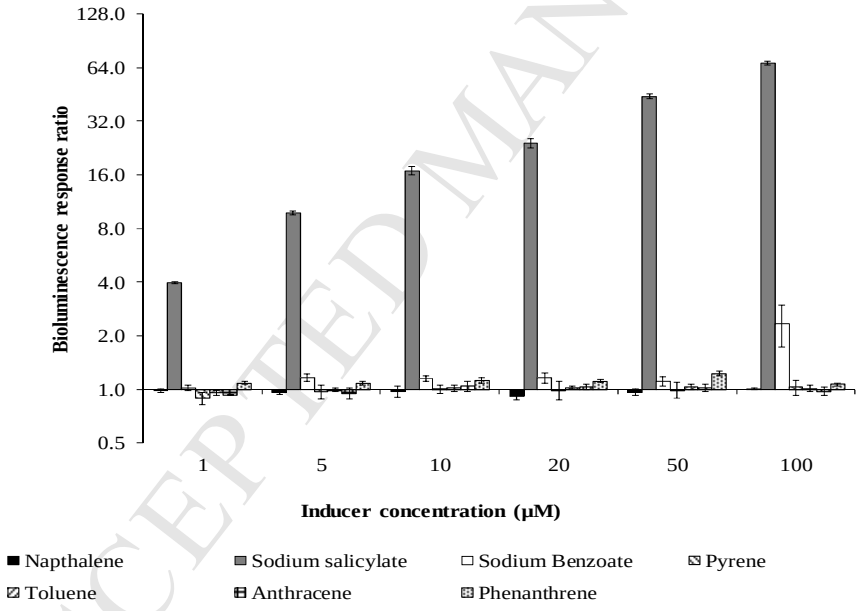

65

66 **(B)**

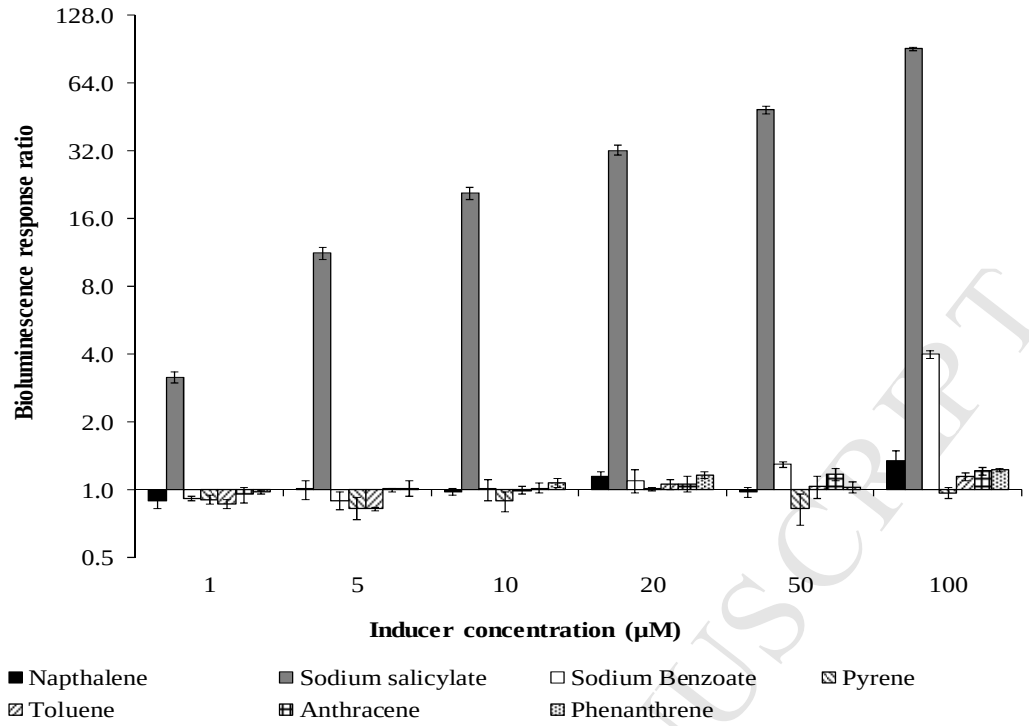

(C)

Fig. 4. The response of ADPWH_Nah (A), ADPWH_1274 (B) and ADPWH_lux (C) to various PAHs and interfering substances. The three whole-cell bioreporters had the same responsive pattern to sodium salicylate and sodium benzoate, illustrating their similar stimulation mechanisms of *salAR* operon activation by salicylate or benzoate. ADPWH_Nah exhibited the unique positive response to naphthalene, but no response in the presence of pyrene, toluene, anthracene, and phenanthrene. (Asterisks indicate significant difference response compared bioreporter A to B/C)

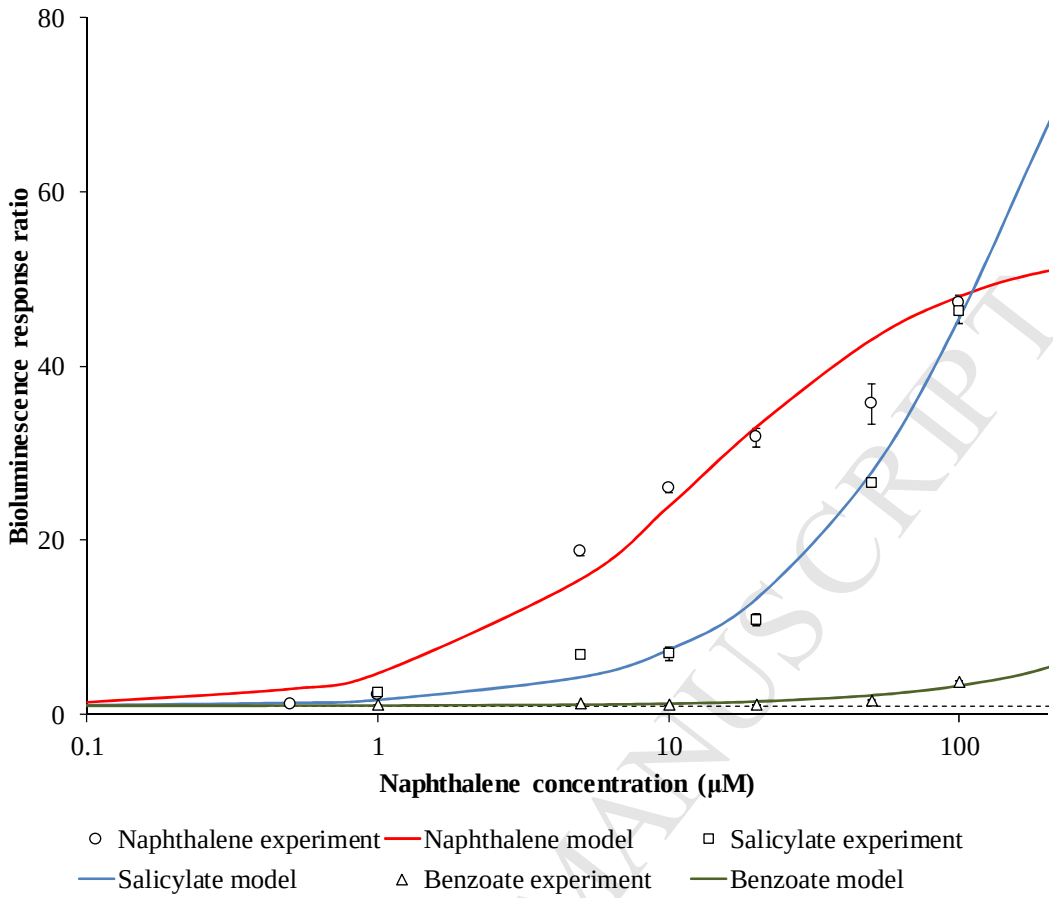

Fig. 5. The model simulation of ADPWH_Nah's response to different concentrations of naphthalene (R^2=0.98, RMSE=3.38), sodium salicylate (R^2=1, RMSE=1.58), and sodium benzoate (R^2=1, RMSE=0.33). The experimental data were the average bioluminescence response ratios of ADPWH_Nah between 200 and 240 min induction.

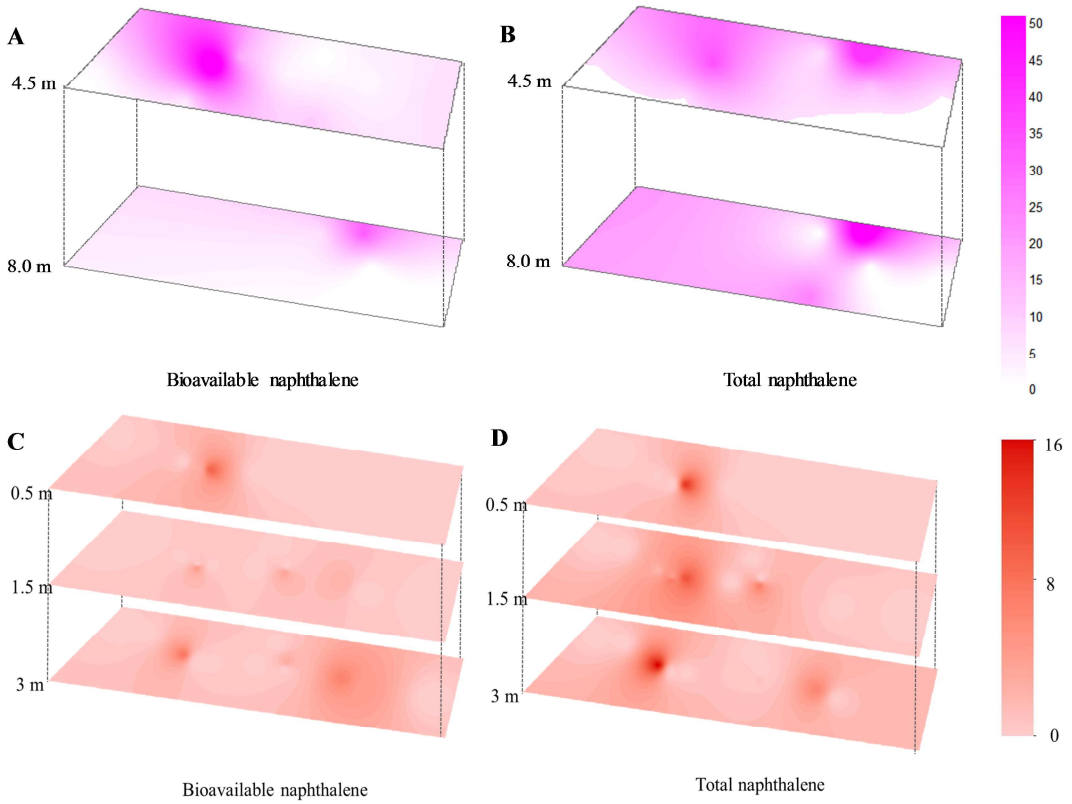

Fig. 6. Naphthalene contamination in groundwater and soil. The bioreporter-estimated naphthalene in groundwater (μg/L) (A) and soil (mg/kg) (C) were analyzed by whole-cell bioreporter, and calculated from the model simulation. The total naphthalene in groundwater (μg/L) (B) and soil (mg/kg) (D) were obtained by GC/MS. The contaminant distribution was plotted by Surfer 8.0 (Golden Software). A positive relationship was found between bioreporter-estimated naphthalene and total naphthalene in groundwater (Pearson coefficient is 0.548 and p value<0.05), and soil (Pearson coefficient is 0.740 and p value<0.05).

Highlights:

- We constructed a novel bioreporter, for rapid detecting naphthalene.
- It suggested a new concept for multiple PAHs whole-cell bioreporter construction.
- The bioreporter achieved rapid evaluation of naphthalene in real site.